

# The influence of rotation on optical emission profiles of O stars

D. John Hillier,<sup>1\*</sup> Jean-Claude Bouret,<sup>2,3</sup> Thierry Lanz,<sup>4</sup> Joseph R. Busche<sup>5</sup>

<sup>1</sup> Department of Physics and Astronomy & Pittsburgh Particle physics, Astrophysics, and Cosmology Center (PITT PACC), University of Pittsburgh, Pittsburgh, PA 15260, USA

<sup>2</sup> Laboratoire d'Astrophysique de Marseille, CNRS-Université de Provence, Pôle de l'Étoile Site de Château-Gombert, 38, rue Frédéric Joliot-Curie 13388 Marseille cedex 13, France

<sup>3</sup> NASA/Goddard Space Flight Center, Greenbelt, MD 20771, USA

<sup>4</sup> Laboratoire J.-L. Lagrange, UMR 7293, Université de Nice-Sophia Antipolis, CNRS, Observatoire de la Côte d'Azur, Boulevard de l'Observatoire, B.P. 4229, F-06304 Nice cedex 4, France

<sup>5</sup> Wheeling Jesuit University, Wheeling, WV 26003

Accepted . Received

## ABSTRACT

We study the formation of photospheric emission lines in O stars and show that the rectangular profiles, sometimes double peaked, that are observed for some stars are a direct consequence of rotation, and it is unnecessary to invoke an enhanced density structure in the equatorial regions. Emission lines, such as N IV  $\lambda 4058$  and the N III  $\lambda\lambda 4634-4640-4642$  multiplet, exhibit non-standard “limb darkening” laws. The lines can be in absorption for rays striking the center of the star and in emission for rays near the limb. Weak features in the flux spectrum do not necessarily indicate an intrinsically weak feature – instead the feature can be weak because of cancellation between absorption in “core” rays and emission from rays near the limb. Rotation also modifies line profiles of wind diagnostics such as He II  $\lambda 4686$  and H $\alpha$  and should not be neglected when inferring the actual stratification, level and nature of wind structures.

**Key words:** radiative transfer – stars: atmospheres – stars: early-types – line:formation — line: profiles

## 1 INTRODUCTION

Many O stars exhibit rapid rotation that broadens their line profiles. In the absence of a wind, the influence of rotation can be accurately computed by integrating the intensities from the stellar disk with allowance for the projected velocity in the direction of the observer. For convenience, and speed, it is customary to allow for the effects of rotation by convolving the flux spectrum with a rotational broadening function that accounts for limb darkening. This procedure, which assumes that the line profile does not change across the disk (i.e., the continuum and line have the same limb darkening laws) (e.g., Gray 1992), generally works very well. As our own tests have shown, the simple convolution procedure is sufficiently accurate for the majority of photospheric absorption profiles in O stars, although for the most precise work the disk integration procedure should be used.

In general, O stars exhibit a wind which modifies the photospheric H $\alpha$  profile (possibly driving H $\alpha$  into emission) and generates numerous UV P Cygni profiles. Because the wind is extended, and because the rotation rate declines with radius, the simple convolution technique is not valid. In such a case it is necessary to take the 2D structure of the wind into account. In the simplest case one can assume that rotation simply affects the velocity structure

of the wind while maintaining an almost spherical structure, while for rapid rotation it is expected that the density structure will also be altered. How the 2D density structure is altered is very complex, and depends on the rotation rate relative to the critical rotation rate, the rotation rate relative to the terminal wind velocity, and the closeness of the star to the Eddington limit. Depending on their values, it is possible to get either density enhancements in the equatorial or polar flows (Maeder & Meynet 2000). A prolate wind structure is expected unless the number of lines (or more correctly the flux [line] mean opacity) increases sufficiently rapidly towards the equator to overcome the decreasing equatorial flux arising from gravity darkening (e.g., Maeder & Meynet 2000).

In many O stars intense N III  $\lambda 4634-4642$  emission is seen and is used as a criterion to define the so-called “f” class (Walborn 1971; Sota et al. 2011). When resolved, these lines can show a rectangular (or trapezoidal-like) profile<sup>1</sup>, with the stronger components exhibiting a double peaked structure. In the spectra of O supergiants presented by Bouret et al. (2012),  $\zeta$  Pup, HD 16691, and HD 210839 show broad, non-gaussian profiles for the N III multiplet, although HD 15570, HD 163758 and HD 192639 exhibit more gaussian-like profiles. The mechanisms driving the N III lines into

<sup>1</sup> For simplicity we refer to these profiles as non-Gaussian, while other profiles will be referred to as Gaussian, even if they do not exhibit extended wings.

\* E-mail: hillier@pitt.edu

emission have been discussed previously by Rivero González et al. (2011). The dominant mechanism depends on the precise stellar parameters – both continuum fluorescence (e.g., the Swings mechanism, Bruccato & Mihalas 1971) and dielectronic recombination (previously discussed for these lines by Mihalas et al. 1972) can be important. Rivero González et al. (2011) also indicate that the strength of the lines can be influenced by interactions between the N III and O III resonance lines.

In this paper we discuss the profiles of photospheric emission lines in O stars, and show that rotation can produce rectangular-like profiles that often exhibit double-peaked profiles. The phenomena is not restricted to the N III  $\lambda\lambda 4634\text{--}4642$  complex — in  $\zeta$  PupN IV  $\lambda 4058$  and Si IV  $\lambda\lambda 4089, 4116$  also exhibit non-gaussian profiles. We show that the observed line profiles are a direct consequence of the lines being photospheric and being in emission. The lines do not show “classic” limb darkening – rather the intensity distribution across the star can be flat, and may even show limb brightening. In addition, we further examine the influence of rotation on the H $\alpha$  and He II 4686 line profiles. Rotation produces observable effects on the line profiles, and these effects are seen. Because of the influence of rotation on the wind velocity law (which is now 2D) wind line profiles potentially depend on both  $v$  and  $\sin i$  rather than  $v \sin i$ . To model these emission lines on O stars, it is absolutely essential to properly account for the effects of rotation in O stars that exhibit rapid rotation. It is especially true for rapid rotators such as  $\zeta$  Pup which has  $v \sin i \sim 210 \text{ km s}^{-1}$ .

## 2 PREVIOUS WORK

The influence of rotation on O star profiles has been the subject of several different studies. Petrenz & Puls (1996) studied the influence of rotation on H $\alpha$ . Their work was mainly concerned with the influence of rotation on the wind profile. Rotation directly influences the velocity structure (the velocity along a given sight line is not necessarily monotonic) and can potentially alter the density structure of the wind through direct means (as in the wind-compressed disk (WCD) model of Bjorkman & Cassinelli (1993)) or indirectly by introducing a latitudinal variation of temperature and surface gravity which then causes a latitudinal variation of the mass loss rate and the velocity law.

In the work of Petrenz & Puls (1996) emission in H $\alpha$  was significantly modified by the enhancement of density in the equatorial plane arising from the WCD effect. However, this effect was likely substantially overestimated — Owocki et al. (1998) showed that non-radial forces will inhibit both the formation of a wind-compressed disk and a wind-compressed region. As a consequence, the most important influence of rotation on the wind arises from rotation introducing a latitudinal dependence of temperature and surface gravity, but this effect remains relatively small unless  $V_{\text{rot}} > 0.8V_{\text{crit}}$ . Two potentially important effects for wind lines are the decrease of  $V_{\phi}$  with  $r$  which reduces the influence of rotational broadening on wind lines, and the resonance-zone effect which arises because rotation introduces a non-monotonicity in the velocity law along some sightlines (Petrenz & Puls 1996). Given the current uncertainties in our understanding of 1D winds, it is fair to say that the structure of 2D winds, and the azimuthal variation of density and mass-loss, is still very uncertain.

Another study of the influence of rotation on line profiles in O stars was made by Busche & Hillier (2005). They examined a range of profiles, showed that the absorption profiles were adequately modeled via the convolution technique, and confirmed the

important influence of rotation on H $\alpha$  and He II  $\lambda 4686$  line profiles. While the analysis was general, and applied to the whole spectrum, they did not study the formation of photospheric emission lines.

## 3 TECHNIQUE

To study the influence of rotation we use the 2D code developed by Busche & Hillier (2005). This code computes the formal solution (and hence line profiles) for axisymmetric 2D winds. It uses as input 1D opacities and emissivities computed with the 1D formal solution code, CMF\_FLUX (Busche & Hillier 2005). It has been parallelized, and runs efficiently on workstations with multiple processors.

In the present calculation we assume that rotation does not influence the density structure — this assumption is a reasonable first approximation since the rotation rates are less than 50% of the critical rotation rate, and much less than the wind terminal velocities. We also neglect the latitudinal variation of temperature and surface gravity with latitude — these are likely not to have a large effect since the rotational velocity of most O stars is generally a factor of 2 (or more) less than the critical rotational velocity. Following the work of Busche & Hillier (2005) we assume that the star rotates as a solid body below  $20 \text{ km s}^{-1}$ , and that angular momentum about the center of the star is “conserved” at higher velocities (that is,  $V_{\phi} \propto R(V = 20 \text{ km s}^{-1})/r$ ). Following the work of Owocki et al. (1998) we assume non-radial forces inhibit disk formation and hence set the polar velocity component to zero. The last two assumptions only influence the formation of wind lines – they do not affect photospheric lines. For simplicity, we neglect the influence of rotation on the non-LTE populations – such effects are likely weak, and have been discussed by Petrenz & Puls (2000).

## 4 OBSERVATIONS AND MODEL

To illustrate the influence of rotation we use  $\zeta$  Puppis which is a fast rotator with  $v \sin i \sim 210 \text{ km s}^{-1}$ . This star has been extensively analyzed, most recently by Bouret et al. (2012). Najarro et al. (2011) have also extensively analyzed this star and obtained similar results. The model parameters we adopt are from the paper of Bouret et al. (2012), and are as follows:  $T_{\text{eff}} = 40\,000 \text{ K}$ ,  $\log g_c = 3.64$  (centrifugally corrected value of  $\log g$ ),  $\dot{M} = 2.0 \times 10^{-6} M_{\odot} \text{ yr}^{-1}$ ,  $\log L/L_{\odot} = 5.91$ ,  $f_{\infty} = 0.05$ ,  $v_{\text{cl}} = 100 \text{ km s}^{-1}$ ,  $N(\text{He})/N(\text{H}) = 0.16$ ,  $Z(\text{C}) = 2.86 \times 10^{-4}$ ,  $Z(\text{N}) = 1.05 \times 10^{-2}$  and  $Z(\text{O}) = 1.30 \times 10^{-3}$  ( $Z$  denotes mass fraction).<sup>2</sup>  $f_{\infty}$  and  $v_{\text{cl}}$  control the clumping in the wind and have little influence on the photospheric profiles. For illustration purposes, we use the same observational data (which covers 3800 to 8800 Å at a resolution of 48,000 and a signal-to-noise in excess of 100 to 1 per pixel) as presented in that paper.

$\zeta$  Puppis is an ideal candidate for the study. Its parameters are well known (except for uncertainties induced by the uncertainty in its distance; see discussion in Schilbach & Röser 2008), and from variability studies it is most likely observed edge on (i.e., rotation axis perpendicular to line of sight; Howarth et al. (1995)). It exhibits several emission lines such as N IV  $\lambda 4058$ , N III  $\lambda\lambda 4634\text{--}4642$ , and Si IV  $\lambda\lambda 4089, 4116$  that show non-gaussian profiles – generally rectangular but possibly exhibiting enhanced emission

<sup>2</sup> Expressed as number fractions:  $N(\text{C})/N(\text{H}) = 4.0 \times 10^{-5}$ ,  $N(\text{N})/N(\text{H}) = 1.2 \times 10^{-3}$  and  $N(\text{O})/N(\text{H}) = 1.4 \times 10^{-4}$ .

near the extremes of the emission profile. Further, C IV 5801, 5812 exhibits complex profiles while both H $\alpha$  and He II are in emission.

Observed profiles for a selection of lines in  $\zeta$  Pup are shown in Fig. 1. Also shown are the profiles obtained from a simple convolution of the 1D model flux with the rotation profile, and the profile computed from a full integration of the intensities across the disk of the star (hereafter disk profiles). For simplicity we adopted a macroturbulent velocity<sup>3</sup> of  $0 \text{ km s}^{-1}$  (Bouret et al. 2012 adopted  $90 \text{ km s}^{-1}$ ) and a rotation velocity of  $240 \text{ km s}^{-1}$  (and  $\sin i = 1$ ) to better match the width of the rectangular emission profiles rather than the  $210 \text{ km s}^{-1}$  adopted by Bouret et al. (2012). As readily apparent, the disk profiles generally show much better agreement with the observed profiles than do the profiles obtained through convolution. In particular, N IV  $\lambda 4058$  exhibits a double peaked profile, as observed. Similarly, the N III lines show rectangular profiles. Lines affected by the wind also show improvements in profile shapes — He II 4686 exhibits evidence for “absorption” on the blue side which is clearly seen in the observation but is not present in the profiles created by convolution. Profiles computed assuming a higher rotation velocity of  $480 \text{ km s}^{-1}$  and  $\sin i = 0.5$  so that  $v \sin i = 240$  are essentially identical to those computed using the lower rotation velocity. In reality, since the wind and star properties would change with such a high rotation rate, the profiles would not be identical.

It is not surprising that the convolution procedure does not work well for H $\alpha$  and He II  $\lambda 4686$ . Both lines are significantly influenced by the wind, and line transfer in the wind will be significantly affected by the presence of rotation.

From Fig. 1 it is apparent that predicted disk profiles do not agree precisely with those observed. This likely arises because of errors in the adopted stellar parameters and abundances, errors in the atomic data, and missing physics. A full discussion of the uncertainties associated with the parameters of  $\zeta$  Pup has been given by Bouret et al. (2012). As the purpose of this paper is to understand the physics giving rise to the observed rectangular profiles, and to re-examine the influence of rotation, we do not attempt to readjust model parameters. We note, for example, that the absorption associated with H $\alpha$  is sensitive to the radial variation of clumping with radius (Hillier et al. 2003; Puls et al. 2006; Najarro et al. 2011) and porosity effects (Sundqvist et al. 2011). Our own work on O supergiants (Bouret et al. 2012) also shows that it is model sensitive (it varies significantly when the stellar parameters are varied over their error range).

To understand the observed emission line profile, and why convolution does not work we consider N IV  $\lambda 4058$ . In Fig. 2 we show the intensity variation at line center (no rotation) and in the adjacent continuum as a function of impact parameter. As apparent, the intensity variation in the continuum and the line is very different — the continuum shows “classic” limb darkening, while the intensity in N IV  $\lambda 4058$  is almost flat. Since the “limb darkening laws” for the continuum and line differ substantially, we cannot use the simple convolution procedure to obtain the profile when the star is rotating. Rather, the observed line profile must be obtained by integrating the intensities across the disk.

From Fig. 2 it is also apparent that the wind makes relatively little contribution to N IV  $\lambda 4058$ . N IV  $\lambda 4058$  is a photospheric emission line, and is in emission because of non-LTE effects. In

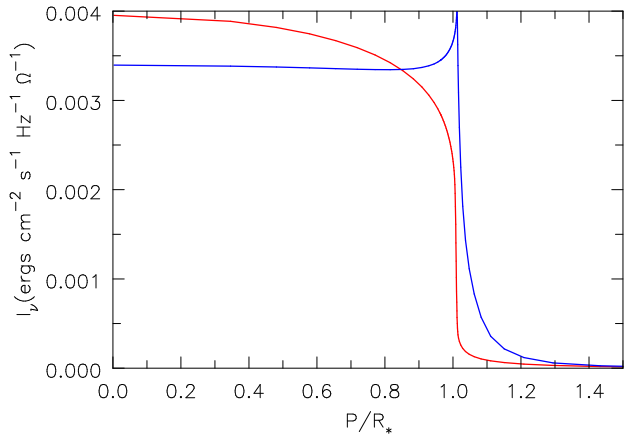


**Figure 2.** Illustration of the “limb darkening law” for the N IV  $\lambda 4058$  line at line center (blue curve) and the adjacent continuum ( $\lambda 4056$ ; red curve). The continuum shows a classic limb-darkening law. Conversely, because of non-LTE effects, the N IV  $\lambda 4058$  line intensity is almost constant across the star and brightens near the limb.

Fig. 3 we illustrate the origin of the N IV  $\lambda 4058$  as a function of the Rosseland mean optical depth, and velocity. This diagram also confirms that N IV  $\lambda 4058$  is photospheric — the bulk of the line originates inside  $10 \text{ km s}^{-1}$ .

To better understand why N IV  $\lambda 4058$  exhibits a non-gaussian profile we can examine the center-to-limb variation of the intensities as a function of velocity, and this is shown in Fig. 4 for a range of impact parameters. As readily apparent, the N IV  $\lambda 4058$  profile shows substantial variation with impact parameter — for the core ray the line is in absorption while it is strongly in emission near the limb. Since the observed flux is a complicated weighting of the intensities, we illustrate in Fig. 5 the growth in the spectrum with impact parameter. When integrated over the inner core rays (for all azimuthal angles) we see an absorption line spectrum, but as we extend the integration zone to higher impact parameters we begin to see emission, and eventually we get the double peaked profile, similar to what is observed.

Another line that exhibits a rectangular-shaped profile is N III  $\lambda 4634$ . While the line is in emission at all impact parameters (Fig. 6), it is much more in emission at the limb. It is this enhanced emission from “large” impact parameters that changes the profile shape from Gaussian to rectangular (Fig. 7).

To complete our study we illustrate two other lines. The first is C IV  $\lambda 5801$  which shows an absorption component together with extended wind emission. In many O stars this line is very difficult to model, being sensitive to both line blanketing (Bouret et al. 2012) and model parameters. This line, like N IV  $\lambda 4058$ , is in absorption for core rays (Fig. 8), but in emission for rays near the limb. However, in contrast to N IV  $\lambda 4058$ , the line remains in absorption longer (i.e., to higher impact parameters) before switching to emission. The central part of the line in the full spectrum thus remains in absorption (Fig. 9). Careful study of Fig. 9 reveals extended emission line wings arising from the wind. Given the transition from absorption to emission as we move to higher impact parameters, and since what we observed is a weighted sum of this variation, it is not surprising that the line is model sensitive.

From Fig. 1 we see that the C IV absorption profiles are narrower than what one would predict based of the rotation rate of the stars. Although not so evident in the current model, disk profiles for C IV  $\lambda 5801$  are generally narrower than those obtained

<sup>3</sup> The use of a (constant) macroturbulent velocity is, of course, another approximation which will modify line profiles and hence influence conclusions that can be drawn from them.

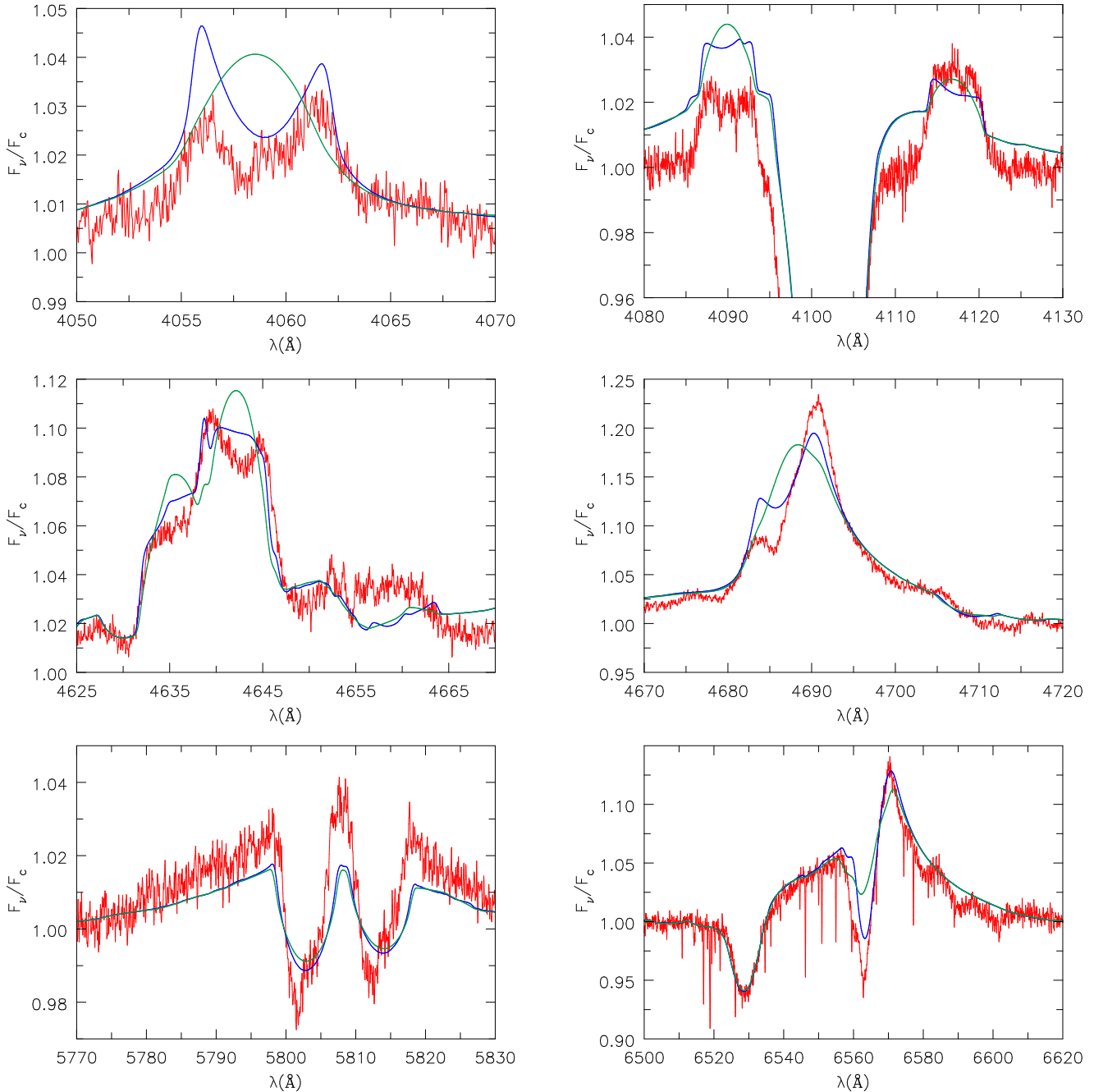


**Figure 1.** Illustration of a sample of line profiles. The red curve shows the spectrum of  $\zeta$  Pup, the blue curve shows the spectrum computed using the formal integral of the 2D model with  $v \sin i = 240 \text{ km s}^{-1}$ , and the green curve shows profiles obtained through convolution of the 1D-flux spectrum with  $v \sin i = 240 \text{ km s}^{-1}$ . From left to right, top to bottom we show N IV  $\lambda 4058$ , Si IV  $\lambda\lambda 4089, 4116$ , N III  $\lambda\lambda 4634-4640-4642$ , He II  $\lambda 4686$ , C IV  $\lambda\lambda 5081, 5812$  and H $\alpha$ . In all cases the profiles computed with the 2D model show better agreement than the profiles obtained via convolution with that observed. In particular notice the distinct non-gaussian profiles associated with N IV  $\lambda 4058$ , Si IV  $\lambda 4089, 4116$ , and N III  $\lambda\lambda 4634-4640-4642$ . On this plot wavelengths are vacuum, but we use air wavelengths (as is the usual practice) when identifying lines.

via convolution. To get a better match for the present model would require stronger C IV absorption for core rays, and (possibly) enhanced emission for the limb rays. Because the absorption is preferentially confined to the core rays, the full disk absorption profiles would be narrower than for pure absorption lines.

The final line studied is He II  $\lambda 4686$ . This line exhibits strong emission, but in  $\zeta$  Pup (and some other stars) it shows a notch on the blue side. As shown in Fig. 1, this notch can be explained by correctly accounting for the effects of rotation. Like N IV  $\lambda 4058$  and

C IV  $\lambda 5801$  this line also transitions from absorption for low impact parameters to emission for high impact parameters (Fig. 10). However there are important distinctions in its behavior from these two lines. First, we see extended absorption to the blue, arising from the stellar wind. Second, wind emission is very important and is what drives the line into emission (Fig. 11).

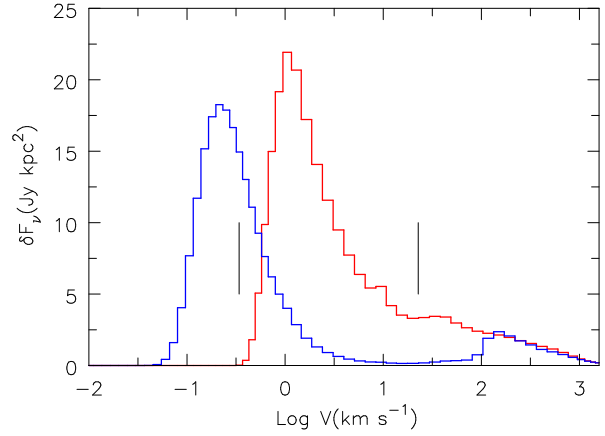
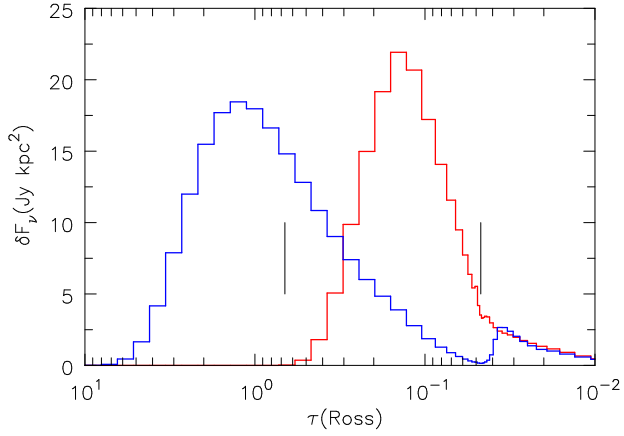


**Figure 3.** Illustration of the origin of the N IV  $\lambda 4058$  line at line center (blue curve) and the adjacent continuum ( $\lambda 4057$ ; red curve) in  $\tau$  and (radial) velocity space for a 1D non-rotating star. Each data value (bin) provides the contribution to the total flux from that pixel – the total flux is the sum over all pixels. The two vertical lines in each figure indicate the location of  $\tau_{\text{Ross}} = 2/3$  (left line) and the location where the wind velocity matches the isothermal sound speed ( $\sim 23 \text{ km s}^{-1}$ ).

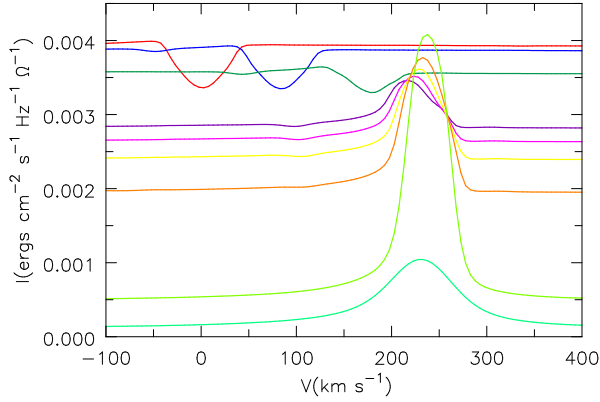


**Figure 4.** Intensity along the equator as a function of impact parameter for N IV  $\lambda 4058$ . The rotation velocity is  $240 \text{ km s}^{-1}$ . From top to bottom we show the intensity for  $p/R_* = 0.0, 0.039, 0.733, 0.965, 0.983, 0.997, 1.007, 1.0127, 1.062$  and  $100 (=R_{\text{max}}/R_{\text{star}})$ . Notice how the line is in absorption near the center of the star but goes into emission near the limb. We only show the curves for half the star – curves for the equatorial region rotating towards the observer are similar (although not identical) to those shown above.

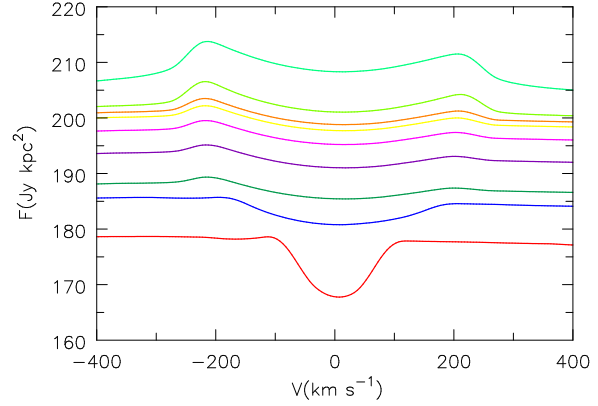


**Figure 5.** Plot showing the spectrum computed by integrating from  $p = 0$  to  $p(i)$  where  $p(i)/R_* = 0.039, 0.733, 0.965, 0.983, 0.997, 1.007, 1.0127, 1.062$  and  $100 (=R_{\text{max}}/R_{\text{star}})$ . The curves for  $p(i)/R_* = 0.039$  (bottom) and  $p(i)/R_* = 0.733$  have been scaled upwards by factors of 7.5 and 1.7, respectively. These plots, together with Fig. 4, illustrate how the observed profile is a complicated blend of absorption and limb emission.

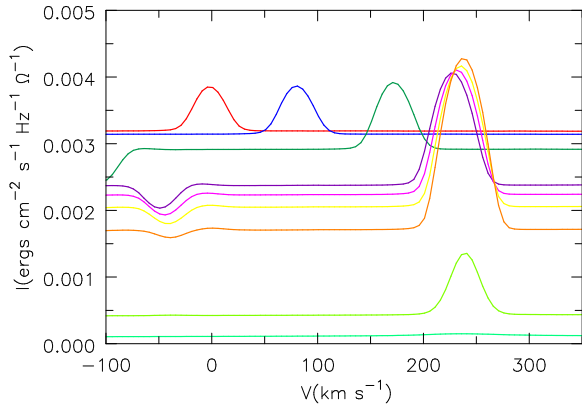


**Figure 6.** As for Fig. 4 but illustrating N III  $\lambda 4634$ . The strength of the emission relative to the continuum is significantly enhanced towards the limb of the star.

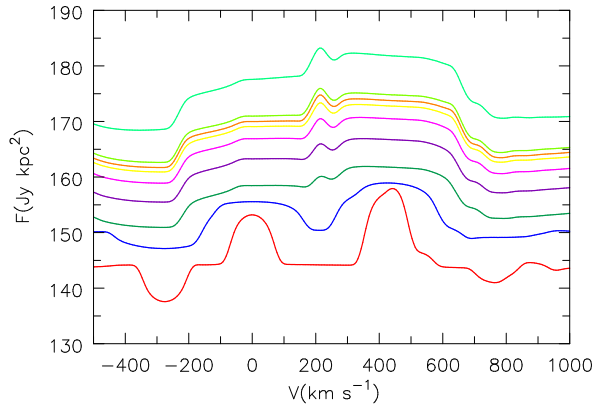


**Figure 7.** As for Fig. 5 but illustrating N III  $\lambda 4634$ . At  $\sim 400 \text{ km s}^{-1}$  we see a blend of two other N III lines ( $\lambda\lambda 4641, 4642$ ) that belong to the same multiplet.

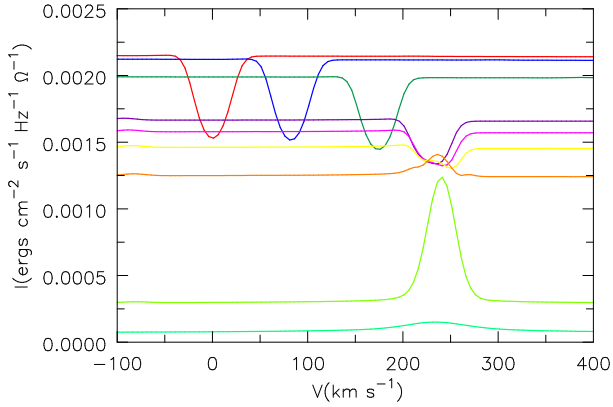


**Figure 8.** As for Fig. 4 but illustrating C IV  $\lambda 5801$ . The strength of the emission relative to the continuum is significantly enhanced towards the limb of the star.

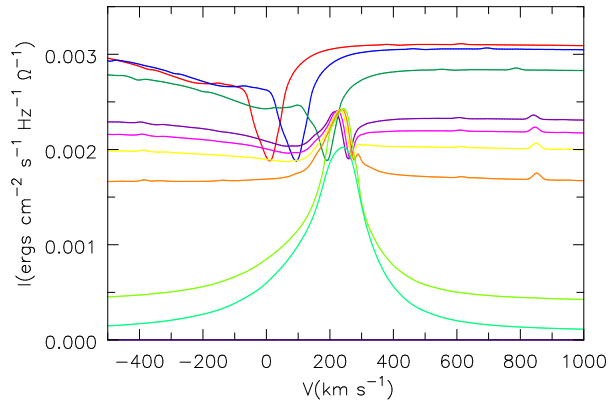


**Figure 10.** As for Fig. 4 but illustrating He II  $\lambda 4686$ . Because of the wind, these profiles exhibit absorption in the blue.

## 5 CONCLUSION

We have demonstrated that rotation alone can explain the rectangular profiles, sometimes double-peaked, that are observed for some optical emission lines in O stars. It is not necessary to invoke departures of the density structure from spherical symmetry to explain these profiles. To properly compute the emission line profiles, it is necessary to integrate the intensities across the rotating stellar disk – the classic convolution of the flux does not work because the line profiles vary substantially across the stellar disc (i.e., with impact parameter). In some cases the line is in absorption for rays striking the center of the star, while it is strongly in emission for rays near the limb. For N IV  $\lambda 4058$  in  $\zeta$  Pup, the observed weak double peaked profile is actually a result of near perfect cancellation between absorption at low impact parameters, and emission at high impact parameters. This illustrates that the variation in intensity with impact parameter can provide additional insights into line formation.

From their study of the N III lines in HD 16691, De Becker et al. (2009) concluded that the lines arise from close to the star in a large scale corotating structure. While we confirm that rotation is crucial in explaining the observed line shapes, we find that the N III lines are primarily of photospheric origin in these supergiants and that rotation alone can explain their observed shapes.

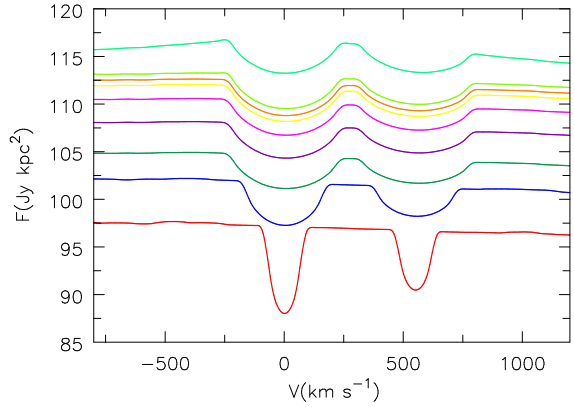


**Figure 9.** As for Fig. 5 but illustrating C IV  $\lambda 5801$ . At  $\sim 500$  km  $s^{-1}$  we see the other component (C IV  $\lambda 5812$ ) of the doublet. In the top spectrum an additional broad emission component arising from the wind is evident.

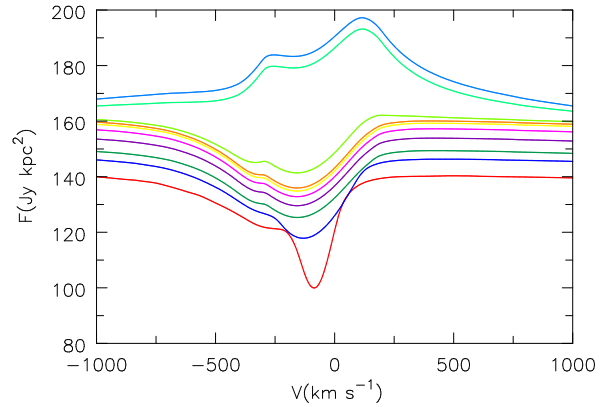


**Figure 11.** As for Fig. 5 but illustrating He II  $\lambda 4686$ . The additional curve (second from top) is for  $p/R_* = 2.513$ , and was included because this line is significantly influenced by wind emission.

For most analyses it is adequate to use the normal convolution technique when modeling absorption lines. However, there are subtle differences between disk profiles, and the profiles obtained with convolution, and these could be important when using absorption lines to study line asymmetries and the possible influence of the velocity field at the base of the wind. Following a suggestion by Francisco Najarro, and due to the intense interest with the mass of the most massive stars, we also ran a model for R136a3, which was found by Crowther et al. (2010) to have an initial mass of  $\sim 165 M_\odot$  and a  $v \sin i \sim 200$  km  $s^{-1}$ . Profiles computed using a 2D model to take into account rotation showed only small differences from profiles computed using the convolution technique, and are too small to significantly affect conclusions drawn by Crowther et al. (2010).

Although already well known, we also highlighted the influence rotation has on main optical wind diagnostics – H $\alpha$  and He II  $\lambda 4686$ . While the correct allowance for rotation does not fundamentally alter the line strength (and hence, for example, inferred mass-loss rates) it does significantly alter the line profile. This is of crucial importance – it means that H $\alpha$  and He II  $\lambda 4686$  emission line profiles in rapidly rotating O stars cannot be used to infer variations in clumping with distance and the importance of velocity-porosity unless rotation is accurately taken into account. Further,

rotation will influence the accuracy of parameters, such as  $\beta$  (in the classic wind-law  $v(r) = (1 - r/R_{\text{ref}})^{\beta}$ ).

The correct treatment of rotation is also important for UV resonance lines formed in the wind. As photospheric lines can influence the resonance line profiles, it is important to take rotation into account. However, a simple convolution overestimates the effect of rotation on the wind lines and can adversely affect estimates of the terminal velocity, and microturbulence within the wind.

Since it is relatively easy to treat the gross influence of rotation accurately, this should become the norm in future studies of O stars. Issues related to the influence of rotation on the azimuthal density structure, and the dependence of clumping parameters on rotation, will require further studies.

## ACKNOWLEDGEMENTS

DJH acknowledges support from NASA ADP Grant: NNG04GC81G, STScI theory grant HST-AR-11756.01.A and HST-AR-12640.01. STScI is operated by the Association of Universities for Research in Astronomy, Inc., under NASA contract NAS5-26555. J.-C. Bouret thanks the French Agence Nationale de la Recherche (ANR) for financial support. The authors thank the referee, Joachim Puls, for his suggestions, and his careful reading of the paper. The authors would also like to thank Francisco Najarro for comments on a draft of the paper.

## REFERENCES

- Bjorkman, J. E. & Cassinelli, J. P. 1993, *ApJ*, 409, 429  
 Bouret, J.-C., Hillier, D. J., Lanz, T., & Fullerton, A. W. 2012, *A&A*, submitted  
 Bruccato, R. J. & Mihalas, D. 1971, *MNRAS*, 154, 491  
 Busche, J. R. & Hillier, D. J. 2005, *AJ*, 129, 454  
 Crowther, P. A., Schnurr, O., Hirschi, R., Yusof, N., Parker, R. J., Goodwin, S. P., & Kassim, H. A. 2010, *MNRAS*, 408, 731  
 De Becker, M., Rauw, G., & Linder, N. 2009, *ApJ*, 704, 964  
 Gray, D. F. 1992, *The observation and analysis of stellar photospheres*. (Cambridge University Press)  
 Hillier, D. J., Lanz, T., Heap, S. R., Hubeny, I., Smith, L. J., Evans, C. J., Lennon, D. J., & Bouret, J.-C. 2003, *ApJ*, 588, 1039  
 Howarth, I. D., Prinja, R. K., & Massa, D. 1995, *ApJL*, 452, L65  
 Maeder, A. & Meynet, G. 2000, *A&A*, 361, 159  
 Mihalas, D., Hummer, D. G., & Conti, P. S. 1972, *ApJL*, 175, L99  
 Najarro, F., Hanson, M. M., & Puls, J. 2011, *A&A*, 535, A32  
 Owocki, S. P., Cranmer, S. R., & Gayley, K. G. 1998, *Ap&SS*, 260, 149  
 Petrenz, P. & Puls, J. 1996, *A&A*, 312, 195  
 —. 2000, *A&A*, 358, 956  
 Puls, J., Markova, N., Scuderi, S., Stanghellini, C., Taranova, O. G., Burnley, A. W., & Howarth, I. D. 2006, *A&A*, 454, 625  
 Rivero González, J. G., Puls, J., & Najarro, F. 2011, *A&A*, 536, A58  
 Schilbach, E. & Röser, S. 2008, *A&A*, 489, 105  
 Sota, A., Maíz Apellániz, J., Walborn, N. R., Alfaro, E. J., Barbá, R. H., Morrell, N. I., Gamen, R. C., & Arias, J. I. 2011, *ApJS*, 193, 24  
 Sundqvist, J. O., Puls, J., Feldmeier, A., & Owocki, S. P. 2011, *A&A*, 528, A64  
 Walborn, N. R. 1971, *ApJS*, 23, 257